Acta Pharmaceutica Sinica B 2024;14(6):2567−2580

Chinese Pharmaceutical Association
Institute of Materia Medica, Chinese Academy of Medical Sciences

Acta Pharmaceutica Sinica B

www.elsevier.com/locate/apsb
www.sciencedirect.com

ORIGINAL ARTICLE

Carrimycin inhibits coronavirus replication by decreasing the efficiency of programmed −1 ribosomal frameshifting through directly binding to the RNA pseudoknot of viral frameshift-stimulatory element

Hongying Li[a,†], Jianrui Li[a,b,†], Jiayu Li[a], Hu Li[a,c], Xuekai Wang[a], Jing Jiang[a], Lei Lei[a], Han Sun[a], Mei Tang[a], Biao Dong[a,c], Weiqing He[c], Shuyi Si[c], Bin Hong[c], Yinghong Li[b], Danqing Song[b], Zonggen Peng[a,b,c,*], Yongsheng Che[c,*], Jian-Dong Jiang[a,b,c,*]

[a]*CAMS Key Laboratory of Antiviral Drug Research, Institute of Medicinal Biotechnology, Chinese Academy of Medical Sciences & Peking Union Medical College, Beijing 100050, China*
[b]*Beijing Key Laboratory of Antimicrobial Agents, Institute of Medicinal Biotechnology, Chinese Academy of Medical Sciences & Peking Union Medical College, Beijing 100050, China*
[c]*Key Laboratory of Biotechnology of Antibiotics, the National Health and Family Planning Commission (NHFPC), Institute of Medicinal Biotechnology, Chinese Academy of Medical Sciences & Peking Union Medical College, Beijing 100050, China*

Received 18 October 2023; received in revised form 8 January 2024; accepted 4 February 2024

KEY WORDS

Carrimycin;
Coronavirus;
Broad-spectrum antiviral activity;
Programmed −1 ribosomal

Abstract The pandemic of SARS-CoV-2 worldwide with successive emerging variants urgently calls for small-molecule oral drugs with broad-spectrum antiviral activity. Here, we show that carrimycin, a new macrolide antibiotic in the clinic and an antiviral candidate for SARS-CoV-2 in phase III trials, decreases the efficiency of programmed −1 ribosomal frameshifting of coronaviruses and thus impedes viral replication in a broad-spectrum fashion. Carrimycin binds directly to the coronaviral frameshift-stimulatory element (FSE) RNA pseudoknot, interrupting the viral protein translation switch from ORF1a to ORF1b and thereby reducing the level of the core components of the viral replication and transcription complexes.

*Corresponding authors.
E-mail addresses: pumcpzg@126.com (Zonggen Peng), ysche@imb.cams.cn (Yongsheng Che), jiang.jdong@163.com (Jian-Dong Jiang).
[†]These authors made equal contributions to this work.
Peer review under the responsibility of Chinese Pharmaceutical Association and Institute of Materia Medica, Chinese Academy of Medical Sciences.

https://doi.org/10.1016/j.apsb.2024.02.023

frameshifting;
RNA pseudoknot;
Antiviral agent;
RNA target;
Synergistic inhibitory effect

Combined carrimycin with known viral replicase inhibitors yielded a synergistic inhibitory effect on coronaviruses. Because the FSE mechanism is essential in all coronaviruses, carrimycin could be a new broad-spectrum antiviral drug for human coronaviruses by directly targeting the conserved coronaviral FSE RNA. This finding may open a new direction in antiviral drug discovery for coronavirus variants.

1. Introduction

The pandemic of severe acute respiratory syndrome coronavirus 2 (SARS-CoV-2) and the potential threat of other human coronaviruses (hCoVs) calls for broad-spectrum and effective antivirals[1]. Fortunately, since the outbreak of coronavirus disease 2019 (COVID-19), several drugs have been approved for antiviral therapy to treat COVID-19 with emergency use authorization, including antibody antivirals targeting viral entry and chemical drugs targeting viral replicases, such as the RNA-dependent RNA polymerase (RdRp) inhibitors remdesivir, molnupiravir, azvudine, deuremidevir hydrobromide and the 3C-like protease ($3CL^{pro}$) inhibitor nirmatrelvir and ensitrelvir[2–7], as well as the traditional Chinese medicine[8,9]. However, the high variability of viral spike protein greatly affected the efficacy of antibody drugs[10]. Moreover, the current chemical drugs that inhibit viral replicases are not yet satisfactory in the clinic because of their weak antiviral effect and side effects[11–14]. The direct antiviral effect and mechanism of traditional Chinese medicine against coronavirus need to be further demonstrated, although they have shown a certain antiviral effect and possible mechanism of action against viruses[8,9]. Furthermore, the bat origin of hCoVs, the presence of intermediate hosts, and the nature of viral replication, along with human behavior and ecology, suggest that more new coronaviruses may newly emerge in the future and potentially cause epidemic or pandemic diseases worldwide[15]. Therefore, new drugs with potent antiviral efficacy and broad-spectrum activities are highly desirable, especially considering the risk of emerging viruses in the future.

In search for antiviral drugs, we found carrimycin (Fig. 1A) effective against α- and β-coronaviruses, including SARS-CoV-2, in multiple cell lines[16]. Carrimycin is a new macrolide antibiotic approved by the National Medical Products Administration of China in 2019 to treat acute tracheal bronchitis and sinusitis caused by bacterial infections[17]. Due to its promising activity against SARS-CoV-2, carrimycin has been in phase III clinical trials to treat COVID-19 in hospitalized patients in China (ChiCTR2000029867 and ChiCTR2000032242), the United States of America and other countries (NCT04672564)[18,19]. However, the antiviral mechanism of carrimycin remains to be clarified, although carrimycin might inhibit coronaviral infection by targeting post-entry replicative events[16]. In this paper, we found carrimycin decreases the efficiency of programmed −1 ribosomal frameshifting (−1 PRF) by directly binding to RNA pseudoknot of viral frameshift-stimulatory element (FSE) and thus interrupts the viral protein translation switch from ORF1a to ORF1b, consequently inhibiting coronavirus replication and enhancing the antiviral activities of viral replicase inhibitors. The innovative antiviral mechanism of carrimycin might open a new direction to discovering antiviral agents for coronavirus variants.

2. Materials and methods

2.1. Materials

Carrimycin was provided by Professor Wei-qing He (Peking Union Medical College, Beijing, China). Remdesivir (T7766), clarithromycin (T1434), midecamycin (T5037), erythromycin (T1032), roxithromycin (T1151), acetylspiramycin (T1557), azithromycin (T6401), spiramycin (T0819), and azathramycin (T3265) were from Topscience Co., Ltd. (Shanghai, China). Molnupiravir (EIDD-1931, HY-125033) and Nirmatrelvir (PF-07321332, HY-138687) were from MedChemExpress LLC (Shanghai, China). The human embryonic kidney cell line HEK293T and the human hepatocellular carcinoma cell lines Huh7 and Huh7.5 were cultured in Dulbecco's modified Eagle's medium (DMEM, Invitrogen, Carlsbad, CA, USA) supplemented with 10% fetal bovine serum (FBS) and antibiotics (100 U/mL penicillin and 100 mg/mL streptomycin). The human lung cancer cell line H460 was cultured in RPMI 1640 medium (Gibco, Grand Island, NY, USA) supplemented with 10% FBS and antibiotics. Cells were cultured at 37 °C in a 5% CO_2 incubator (Thermo Fisher). Virus strains hCoV-229E (strain VR-740) and hCoV-OC43 (strain VR-1558) were purchased from ATCC and used as surrogates for SARS-CoV-2.

2.2. Test of antiviral activity

Huh7 or H460 cells (1.5×10^4 cells/well) were grown in a 96-well culture plate for 24 h. Then, cells were infected with hCoV-229E or hCoV-OC43 and treated simultaneously with various concentrations of carrimycin. At 72 h, the culture supernatants were replaced with 200 μL of CCK-8 solution in DMEM. Cells were continuously incubated for 2 h at 37 °C in a 5% CO_2 incubator. Absorbance intensity was measured at 450 nm using a microplate reader (Elx808, Bio-Tek Instruments, VT, USA).

Intracellular total RNA in a 12-well culture plate was extracted using the RaPure Total RNA Micro Kit (R4111-03; Magen, China) according to the manufacturer's instructions. Quantitative real-time reverse-transcription polymerase chain reaction (qRT-PCR) was performed with a HiScript II One Step qRT-PCR SYBR Green Kit (Q221-01, Vazyme Biotechnology, Nanjing, China) using the ABI 7500 Fast Real-Time PCR system. Primers 5′-TAAACGAGTCCGGGGCTCTA-3′ and 5′-CGTCA AATGCACG GACACAG-3′ were for the *NSP9* gene, 5′-TGTCGTCT GGGTTGCTGTTGATG-3′ and 5′-AAGGAGCACGGGAGTCAGGTTC-3′ were for the *N* gene, and primers 5′-CGGAGTCAACGGATTTGGTCGTAT-3′ and 5′-AGCCTTCTCCAT GGTGGTGAAGAC-3′ were for the internal control of the *GAPDH* gene.

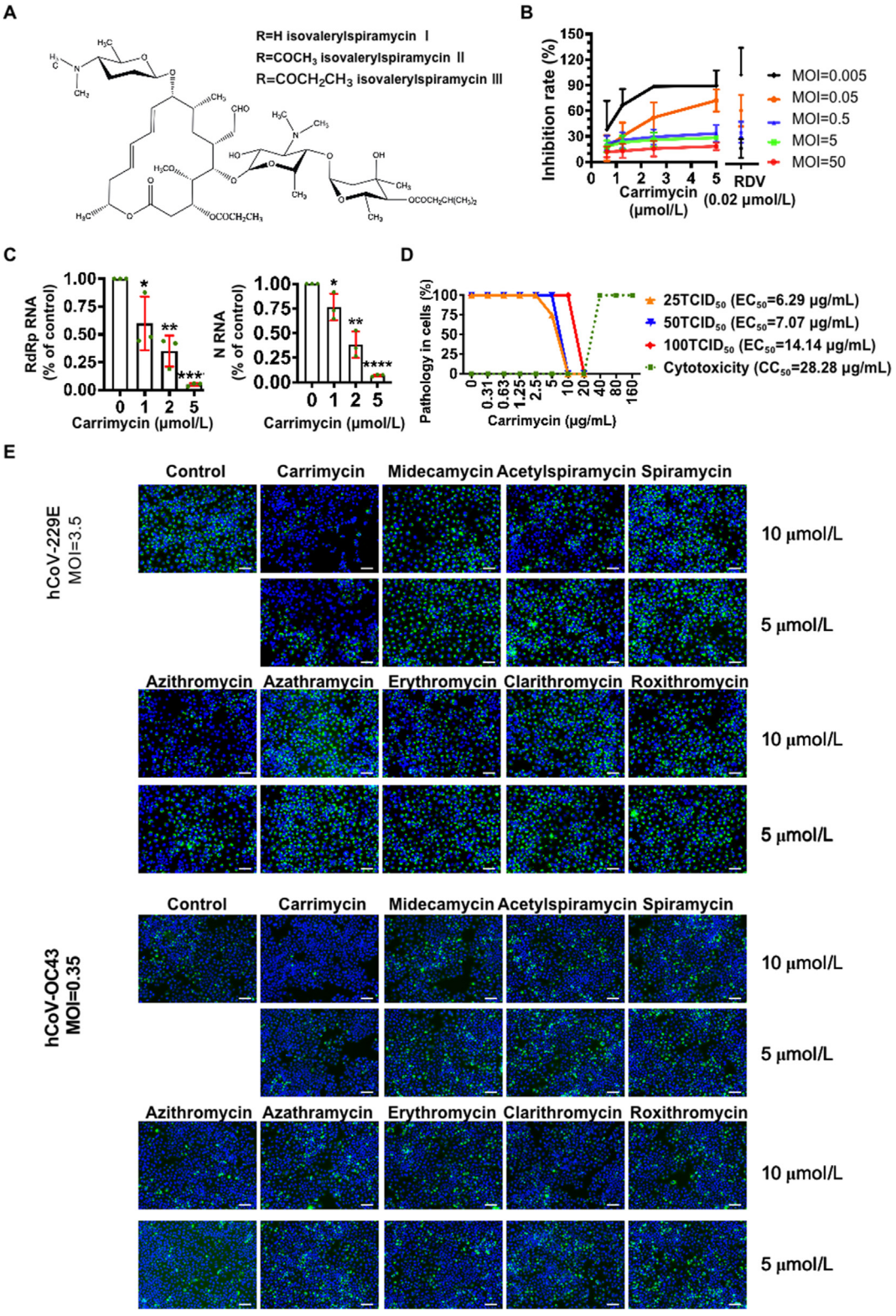

Figure 1 Carrimycin inhibits hCoV replication in cells. (A) The chemical structure of carrimycin. (B) Carrimycin inhibited hCoV-229E replication under a different multiplicity of infection (MOI) detected by CCK-8 assay at 72 h of drug treatment. Remdesivir (RDV 0.02 μmol/L) as a positive control. (C) Carrimycin inhibited hCoV-229E (MOI = 0.03) at the RNA levels quantified by qRT-PCR at 24 h of drug treatment. (D) Carrimycin inhibited the SARS-CoV-2 Omicron strain in Vero-E6 cells (CPE assay). (E) Anti-coronaviral activity of macrolide antibiotics. Viral dsRNA (green) and cell nuclei (blue) in Huh7 cells infected with hCoV-229E and in H460 cells infected with hCoV-OC43 visualized by immunofluorescent staining assay at 24 h of drug treatment. Scale bar: 100 μm. The experiments were carried out three times. *P* values were calculated using Student's *t*-test (mean ± SD, $n = 3$). $^{*}P < 0.05$, $^{**}P < 0.01$, $^{***}P < 0.001$ *vs*. virus control. CC_{50}, 50% cytotoxic concentration; EC_{50}, 50% effective concentration; $TCID_{50}$, 50% tissue culture infective dose.

Huh7 or H460 cells (2×10^4 cells/well) were grown in a 96-well culture plate for 24 h. Cells were infected with hCoV-229E or hCoV-OC43 and treated simultaneously with drugs. At the time points post-infection (2, 4, 6, 8, 10, and 12 h), cells were washed and briefly fixed in PBS with 4% paraformaldehyde (Servicebio, China) for 40 min. The cells were permeabilized in 0.5% Triton X-100 at room temperature for 15 min and then blocked with Odyssey blocking buffer (LI-COR Cat. # 927-40000) for 1 h at room temperature. Cells were incubated with double-stranded RNA (dsRNA) antibody (10010200, SCICONS, Szirák, Hungary) at a dilution of 1:500 for 2 h at room temperature. After washing three times with PBS, samples were reacted with goat anti-mouse IgG (H + L), AF488 conjugate (TransGen Biotech, China; 1:200) for 1 h at room temperature, then incubated with 1 mg/mL DAPI (D8417; Sigma) at a dilution of 1:1000 at room temperature for 20 min. The cells were washed with PBS. Images were taken using a fluorescence microscope (Olympus IX71, Olympus, Japan).

The antiviral effect on the SARS-CoV-2 Omicron strain was analyzed by the cytopathic effect (CPE) method. The experiment was conducted at the Institute of Laboratory Animal Science, Chinese Academy of Medical Sciences, under Biosafety Level 3. Vero-E6 cells (5×10^3 cells/well) were grown in a 96-well culture plate for 24 h. Cells were then incubated with various concentrations of carrimycin or culture mixtures containing the SARS-CoV-2 Omicron strain at different 50% tissue culture infective doses ($TCID_{50}$) of the viruses and various concentrations of carrimycin and pre-incubated for 1 h at 37 °C in a 5% CO_2 incubator. After 72 h at 37 °C in a 5% CO_2 incubator, the CPE of the cells was recorded as yes or no, and the 50% cytotoxic concentration (CC_{50}) and 50% effective concentration (EC_{50}) were calculated by the Reed−Muench method.

2.3. *Ribosome profiling sequencing*

Huh7 cells (25×10^4 cells/well) were grown in a 12-well culture plate for 24 h. Cells were infected with hCoV-229E (MOI = 0.88) and treated with carrimycin. After 24 h, the culture supernatants were replaced with fresh medium containing cycloheximide (0.1 mg/mL) for 1 min. Cells were then washed with ice-cold PBS (containing 0.1 mg/mL cycloheximide) and treated for 10 min with lysis buffer (87.8% Polysome Buffer [20 mmol/L Tris-Cl pH 7.5, 150 mmol/L NaCl, 5 mmol/L $MgCl_2$ and 1 mmol/L DTT], 10% Triton X-100, 1% 100 mmol/L DTT, 1% 1 U/μL DNase I, and 50 mg/mL cycloheximide). Cell lysates were subjected to Ribo-Seq analysis performed by CloudSeq Biotech (Shanghai, China). The library was constructed using the GenSeq Ribo Profile Kit (GenSeq, Inc.). Raw data were generated after sequencing using Illumina NovaSeq 6000, and quality was assessed by calculating Q30 (Q30 ≥ 80%). Low-quality reads, undefined bases, reads with 5′ adapters, reads without 3′ adapters, and insert index was removed. Adapters were trimmed using Cutadapt software. Bowtie (v1.0.0) software was used to compare all the clean reads with sequence comparison databases, and rRNA and tRNA were filtered out to obtain unannotated reads. The clean data from each sample were mapped to the hCoV-229E genome (NC_002645.1) using Tophat 2 software (http://ccb.jhu.edu/software/tophat/index.shtm). RPKMs (reads per kilobase per million mapped reads) of each part of hCoV-229E between each group were calculated, and the efficacy of programmed −1 ribosomal frameshifting is defined as the ratio of ORF1b/ORF1a[20].

2.4. *Proteomics sequencing*

Huh7 cells (125×10^4 cells/well) were plated in 10 cm^2 cell culture dishes (Corning, USA) and cultured for 24 or 32 h. Cells were infected with hCoV-229E (MOI = 0.88) and treated with 5 μmol/L carrimycin. After 24 h, cells were scraped with a cell scraper. Cell lysates were subjected to tandem mass tag (TMT) proteomic sequencing to detect the expression of differentially expressed proteins. MS spectra lists were searched against their species-level UniProt FASTA databases (P0C6X1). TMT proteomic sequencing was carried out by Oebiotech Co., Ltd. (Shanghai, China).

2.5. *Plasmid construction*

A recombinant DNA sequence containing the mCherry gene, the coronaviral FSE (Supporting Information Table S1), and the EGFP gene with the stop codon TAG was synthesized and subcloned into the vector pcDNA3.1(+) to generate a mCherry-viral FSE-EGFP plasmid by Taihe Biotechnology Company (Beijing, China). Plasmids containing truncated FSE of SARS-CoV-2 (Supporting Information Table S2) were constructed using the template (pcDNA3.1(+)-SARS-CoV-2 FSE) by Taihe Biotechnology Company (Beijing, China).

2.6. *−1 PRF efficacy assay in cells*

HEK293T, Huh7, and Huh 7.5 cells (3×10^4 cells/well) were grown in a 96-well culture plate for 24 h. Cells were pretreated with carrimycin at different concentrations for 30 min, then transfected with plasmids (mCherry-SARS-CoV-2 FSE-EGFP) using ExFect transfection reagent (T101-02; Vazyme Biotechnology, Nanjing, China) according to the manufacturer's instructions. At 6 h, the culture supernatants were replaced with culture media containing drugs. After 24 h of transfection, fluorescence intensity (FI) was measured at λ emission ∼507 nm (lambdaexcitation = 488 nm) for EGFP and at λ emission ∼610 nm (λ excitation = 580 nm) for mCherry using a microplate reader EnSpire PerkinElmer (Waltham, MA, USA). Each well was detected 6 × 6 points at the bottom, and the sum of the well was calculated. The inhibition on the efficacy of −1 PRF was calculated using Eq. (1):

$$\text{Inhibition } (\%) = (1-\text{Drug}_{(\text{EGFP/mCherry})}/\text{Model}_{(\text{EGFP/mCherry})}) \times 100 \quad (1)$$

2.7. *−1 PRF efficacy assay in a rabbit reticulocyte lysate*

The plasmid (pcDNA3.1(+)-mCherry-SARS-CoV-2 FSE-EGFP) was digested with restriction endonuclease EcoR I (R0101S, New England Biolabs) at 37 °C for 3 h and then treated with Mung Bean Nuclease (M0250S, New England Biolabs) at 30 °C for 30 min. Products were purified using the Wizard SV Gel and PCR Clean-Up System (Promega, USA) according to the manufacturer's instructions. The purified linear DNA was used for *in vitro* transcription to obtain RNA using the MEGAscript Kit (AM1333; Thermo Fisher). Purified RNA using the Monarch RNA cleanup kit (T2040L, NEB) was used to translate proteins *in vitro* using the RRL TNT T7 Quick Coupled Transcription/Translation system (L1170, Promega) supplemented with 1 mmol/L methionine. The products were detected by Western blot. Briefly, after SDS-PAGE and trans-Membrane, the target proteins were

accordingly probed with the primary antibodies anti-EGFP (1:1000, ab184601, Abcam, UK), anti-mCherry (1:500, 26765-1-AP, Proteintech, China) and GAPDH (1:1000, 10494-1-AP, Proteintech, USA). Images were captured with the ChemiDoc Touch Imaging System (Bio-Rad) using a chemiluminescent reagent (#WBKLS0500, Millipore, Billerica, MA, USA), and intensity was estimated with Image Lab-2 analysis software (Bio-Rad, USA).

2.8. *Rescue experiment*

FSE was amplified from SARS-CoV-2 or h hCoV-NL63 FSE plasmids with the primers (5′-CTTATCGAAATTAATACGACTCAC TATAGGG-3′ and 5′-CCATAGAGCCCACCGCA T-3′) using PCR and Q5 Hot Start High-Fidelity DNA Polymerases (New England Biolabs). Products were purified by gel extraction using the Wizard SV Gel and PCR Clean-Up System (Promega, USA) according to the manufacturer's instructions. The purified DNA was used for *in vitro* transcription using the MEGAscript Kit (AM1333; Thermo Fisher) and the Monarch RNA Cleanup kit (T2040L; NEB) to obtain purified RNA. siRNA targeted at hCoV-229E FSE RNA was designed and synthesized by RIB BIO (China). Huh7 cells (3×10^4 cells/well) seeded for 24 h in 96-well were transfected with RNA using Lipofectamine RNAiMAX Reagent (Thermo Fisher). Non-related RNA (5′-CCUGGUUUUUAAGGAGUGUCGCCAGAGUGCCGCGAA-UGAAAAA-3′) serves as a control. After 8 h, the supernatant was replaced with a normal culture medium, and the cells were infected with hCoV-229E (MOI = 0.01) and simultaneously treated with carrimycin or solvent control. After 72 h of incubation, the cells were stained with a CCK-8 solution, and the absorbance intensity was detected. Inhibition rate was calculated according to Eq. (2):

$$\text{Inhibition rate } (\%) = (OD_{drug} - OD_{virus})/(OD_{cell} - OD_{virus}) \times 100 \quad (2)$$

2.9. *Surface plasmon resonance (SPR) assay*

FSE RNA sequences (Supporting Information Table S1) were amplified from viral FSE plasmids with the primers (5′-CTTATC GAAATTAATACGACTCACTATAGGG-3′ and 5′-CCATAGAG CCCACCGCAT-3′) using PCR and Q5 Hot Start High-Fidelity DNA Polymerases (New England Biolabs). Then, RNAs were transcribed *in vitro* using the MEGAscript Kit (Thermo, AM1333) and attached to a single biotinylated nucleotide at the 3′ terminus of the RNA strand using a Pierce RNA 3′ End Desthiobiotinylation Kit (20163; Thermo Fisher). Non-related FSE RNA (5′-UCCUGCUUCAACAG UGCUUGGACGGAA C-3′-Biotin) was also provided in the kit (20163; Thermo Fisher). The SPR bioassay was developed using a carboxymethylated dextran (CD) chip to bind Streptavidin (250 mg/L, dissolved in 10 mmol/L pH 5.2 sodium acetate buffer) until the amount immobilized reached a maximum. Then 3′ biotinylated RNAs in PBST were injected until the signal reached a maximum. Different concentrations of the compound were tested. SPR data were processed and analyzed using TraceDrawer (Ridgeview Instruments AB). The K_D (mol/L) value was determined using the OneToOne model of kinetic evaluation.

2.10. *RdRp enzymatic activity assay*

The RdRp activity of SARS-CoV-2 was evaluated by fluorometric assay *in vitro*[21]. Briefly, carrimycin was incubated with 2.0 mmol/L SARS-CoV-2 RdRp complex, 1.0 mmol/L self-priming RNA (5′-Biotin-UUUUUUUUUUUUUUUUUUUUUUUUUUUUUUA ACAGGUUCUAGAACCUGUU-3′) and 2 U/μL RNase inhibitor in reaction buffer (20 mmol/L Tris, pH 8.0, 1 mmol/L DTT, 6 mmol/L $MgCl_2$, 10 mmol/L KCl, and 0.01% Triton-X100) for 30 min. To start the reaction, 10 mmol/L ATP was added to the reaction system and incubated at 37 °C for 60 min. Total dsRNA in the reaction product was quantified using the QuantiFluor dsRNA system (Promega) according to the manufacturer's recommendation. The relative activity of SARS-CoV-2 RdRp was reflected in the concentration of dsRNA.

2.11. *$3CL^{pro}$ activity in sandwich-like fluorescence polarization assay*

The $3CL^{pro}$ enzyme activity assay was described previously[22]. In brief, a 30 μL sample of 400 nmol/L Mpro was incubated with various concentrations of carrimycin or PF-07321332 (8 two-fold dilutions) for 35 min at RT in a black 96-well microplate. Then, a 20 μL sample of 60 nmol/L FP substrate (FITC-AVLQSGFRKK-Biotin) was added and incubated for 20 min at room temperature. The FITC-AVLQ peptide-free well was used as a negative control, and the well containing the FITC tracer/avidin binding complex was used as a positive control. After incubation of avidin for 5 min, the mP value was measured. The inhibitory rate of the drugs was calculated using Eq. (3):

$$\text{Inhibition } (\%) = (\mu_{Hit} - \mu_N)/(\mu_p - \mu_N) \times 100 \quad (3)$$

where μ_{Hit}, μ_N, and μ_P represent the average mP values of the tested inhibitor, negative control, and positive control, respectively.

2.12. *Dimethyl sulfate mutational profiling with sequencing (DMS-MaPseq)*

Huh7 cells (40×10^4) were grown in a 6-well culture plate for 24 h. Cells were then infected with hCoV-229E (MOI = 0.88) for 24 h. 10 μmol/L carrimycin was added to the cells and treated for 4 h. Cells were collected with cell scrapers, and RNA was extracted using the HiPure Universal RNA Kit (R4130; Magen). The cDNA converted from DMSO or carrimycin-treated RNAs using TransScript One-Step gDNA Removal and cDNA Synthesis SuperMix kit (AT311; Trans, China) were subjected to sequencing library construction with the GenSeq ssDNA Lib Prep Kit (GenSeq Inc.). DMS-Seq high throughput sequencing and subsequent bioinformatics analysis were all done by CloudSeq Biotech (Shanghai, China). The cDNA was tailed and ligated to 1st adapter and then converted to double-stranded DNA. The double-stranded products were ligated to 2nd adapter and amplified with a PCR mix. After purification, the libraries were sequenced on NovaSeq sequencer (Illumina) with 150 bp paired-end mode according to the manufacturer's instructions. Raw data were generated after sequencing, image analysis, base calling, and quality filtering on the Illumina Novaseq 6000 sequencer. Firstly, Q30 was used to perform quality control. After adaptor-trimming (choose minus strand) and low-quality reads were removed by cutadapt (v1.9.2) software, high-quality reads were generated. Then, these high-quality (≥10 nt) reads were aligned to the genome using bowtie2 software (v2.2.4) with default parameters. Raw counts and coverage counts were calculated by bedtools (v2.24) software and in-house scripts, and then the DMS-ratio (defined as count/coverage) was also calculated. DMS sites were annotated with gene information by bedtools software. The DMS sites were

visualized in IGV software (v2.15.2). After that, we calculated the fold change between the group treated with DMSO and the group treated with carrimycin. The average changes in DMS reactivity upon carrimycin binding were marked.

2.13. Isothermal titration calorimetry (ITC)

The ITC experiment was performed as previously[23]. SARS-CoV-2 FSE RNA sequences were amplified from FSE plasmids using the primers (5′-CTTATCGAAATTAATACGACTCACTATAGGG-3′ and 5′-CCATAGAGCCCACCGCAT-3′) with PCR and Q5 Hot Start High-Fidelity DNA Polymerases (New England Biolabs). Then, RNAs were transcribed *in vitro* using the MEGAscript Kit (Thermo, AM1333). ITC experiments were carried out with a MicroCal PEAQ-ITC (Malvern Instruments) with the sample cell (280 μL) containing 1000 ng/μL RNA and 50 μmol/L carrimycin in the injector syringe (40 μL). After thermal equilibration at 25 °C, an initial 60 s delay, and one initial 0.4 μL injection, 24 serial injections of 1.5 μL at intervals of 150 s and a stirring speed of 800 rpm (MicroCal PEAQ ITC, Malvern) were performed. Raw data were recorded as power (μcal/s) over time (min). The heat associated with each titration peak was integrated and plotted against the corresponding molar ratio of carrimycin and FSE RNA.

2.14. Statistical analyses

Data are expressed as mean ± standard deviation (SD). Student's *t*-test was used to determine the statistical significance of comparisons between the two groups. $P < 0.05$ was considered significant.

3. Results

3.1. Carrimycin inhibits hCoV replication in cells

To address the antiviral mechanism of carrimycin, we first investigated the specific antiviral activity of carrimycin against hCoVs using different detection technologies. Carrimycin inhibited hCoV-229E replication in the Huh7 cells under a diverse multiplicity of infection in a concentration-dependent manner using CCK-8 staining assay (Fig. 1B), and we confirmed the anti-coronavirus effects using qRT-PCR for quantitation of intracellular viral *RdRp* and *N* RNA levels (Fig. 1C), further validating its effectiveness on hCoV replication.

Variants of concern of SARS-CoV-2 were continuously emerging, and the Omicron strain is the currently circulating mutant[24]. Carrimycin also showed inhibitory activity against the SARS-CoV-2 Omicron strain in the Vero-E6 cells at different multiplicities of infection (MOI) (Fig. 1D), hinting that carrimycin is a potential candidate to treat viral infection with the mutant strain of SARS-CoV-2.

Carrimycin is a new structural type of 16-membered macrolide antibiotics[17], which binds onto the bacterial ribosome 50S subunit and thus selectively inhibits bacterial protein synthesis[25]. Hence, we have tested several other 14-, 15-, and 16-membered macrolide antibiotics (Fig. 1E) to learn their antiviral activities. In addition to carrimycin, azithromycin showed positive but weak inhibitory activity against hCoV-229E in the Huh7 cells and hCoV-OC43 in the H460 cells (Fig. 1E), with all of the other tested macrolide antibiotics null of antiviral activity even at the concentration of 10 μmol/L (Fig. 1E), suggesting that the antiviral mechanism of carrimycin is different from that on bacteria and carrimycin might be unique among macrolide antibiotics.

3.2. Carrimycin interrupts the switch of viral protein translation from ORF1a to ORF1b

Our previous results from the time-of-addition experiments using a coronavirus infection system and entry experiments using the pseudovirus infection system suggested that carrimycin efficiently inhibits the infection of hCoVs by targeting one or multiple post-entry replication events[16]. To further learn at which replicative stage carrimycin interrupted during the viral life cycle, we analyzed the antiviral activity of carrimycin with the viral RNA levels within 12 h post infection (hpi). Carrimycin interrupted viral dsRNA synthesis (Fig. 2A and Supporting Information Fig. S1) and decreased the amount of RdRp RNAs (Fig. 2A) in 8 hpi of hCoV-229E when increased intracellular dsRNA was first visualized in the untreated viral control (Fig. 2A and Supporting Information Fig. S1). However, *in vitro*, carrimycin did not display inhibitory activity on viral replicases $3CL^{pro}$ or RdRp (Fig. 2B), hinting that carrimycin might inhibit viral replication before or at the stage of RNA replication.

Then, we analyzed whether carrimycin inhibits the expression of viral non-structural proteins that are essential elements responsible for viral RNA replication. Proteomics sequencing was performed on Huh7 cells infected with hCoV-229E. After 24 or 32 h of treatment with carrimycin, the viral protein ratio of RdRp/$3CL^{pro}$ was decreased compared with the untreated cells (Fig. 2C), suggesting that carrimycin might arrest the switch of protein translation from ORF1a to ORF1b. To further validate the potential mechanism of carrimycin, we carried out ribosome profiling sequencing. Normally, the translation efficiency of ORF1b was about 75% compared with ORF1a (Fig. 2D), which is consistent with the previous report[20]. However, after 24 h of treatment with carrimycin, all viral non-structural proteins were decreased (Fig. 2D). Notably, the protein ratios of ORF1b/ORF1a-translated and RdRp/$3CL^{pro}$ were decreased by carrimycin treatment in a concentration-dependent manner (Fig. 2D), further verifying that carrimycin interrupts the protein translation switch from ORF1a to ORF1b. Because the translation switch is controlled accurately by the programmed −1 ribosomal frameshifting (−1 PRF) event[26], the results hint to us that carrimycin might act at the −1 PRF efficacy.

3.3. Carrimycin decreases the efficiency of −1 PRF of coronaviral RNAs

To determine whether carrimycin negatively affects the efficiency of −1 PRF in coronaviruses, especially SARS-CoV-2, we established a dual fluorescent reporter system (Fig. 3A) according to the principle of −1 PRF event that is controlled accurately by the unique viral frameshift-stimulatory element (FSE) RNA signal[27]. In this system, the fused EGFP at the C-terminal is not translated because of a stop codon in the FSE RNA, but it is translated when it passes the stop codon by the −1 PRF mechanism (Fig. 3A)[27]. Cells were treated with carrimycin and transfected with the plasmid. The efficacy of −1 PRF of SARS-CoV-2 was reduced by carrimycin in the HEK293T, Huh7, and Huh7.5 cells (Fig. 3B) at the 24-h time-point. The inhibitory effect of carrimycin on −1 PRF was similar to that of merafloxacin (Supporting Information Fig. S2), a known −1 PRF inhibitor[28,29]. In the rabbit reticulocyte lysate translation system, which is a cell-free protein synthesis

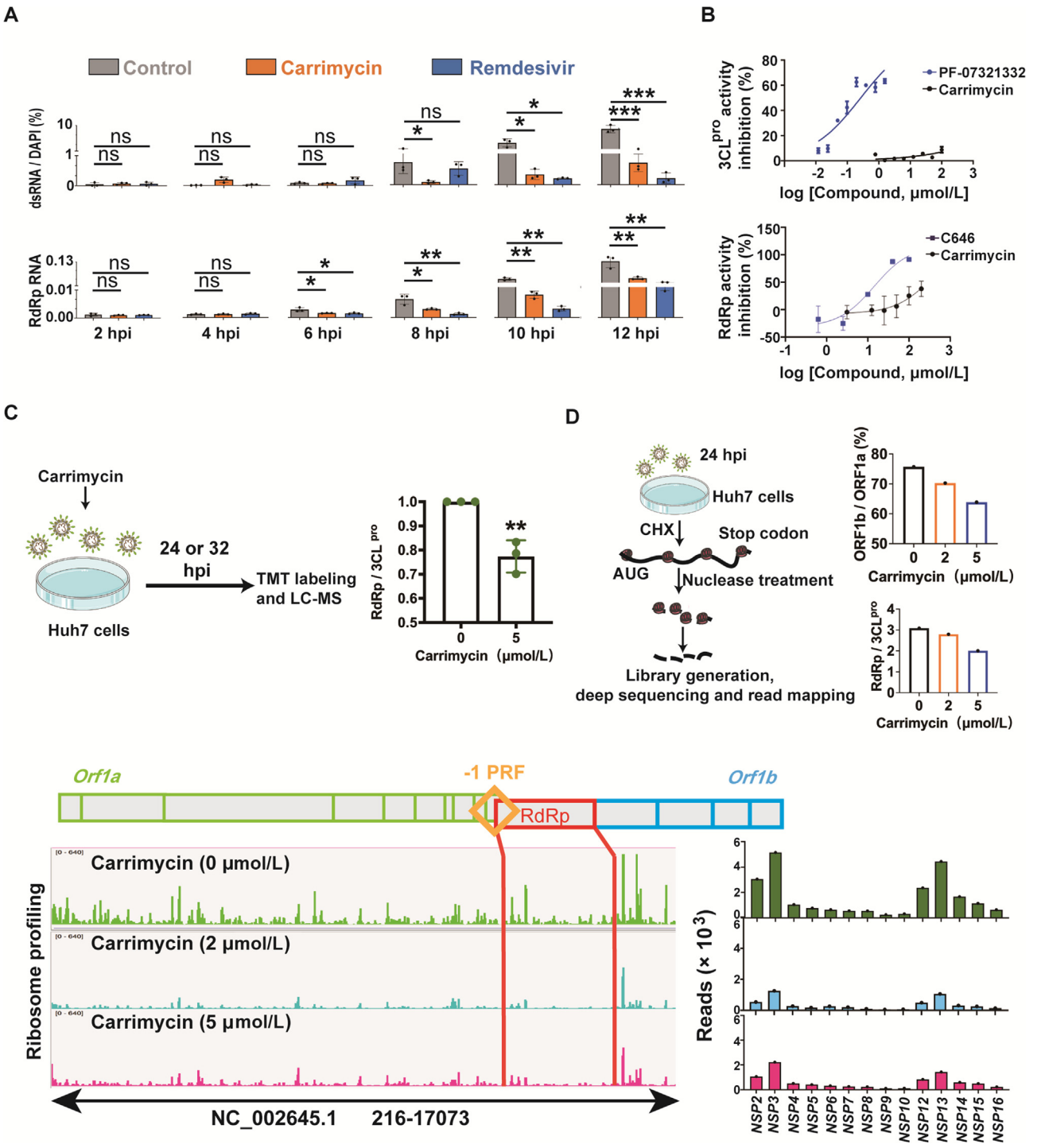

Figure 2 Carrimycin interrupts the viral protein translation switch from ORF1a to ORF1b. (A) Huh7 cells were infected with hCoV-229E (MOI = 5.6) and treated simultaneously with carrimycin (5 μmol/L). Viral dsRNA and cell nuclei were visualized by immunofluorescent staining assay, the ratio of dsRNA/nuclei fluorescent intensity was calculated by Image J, and intracellular RNAs were quantified by qRT-PCR at the indicated hours post-infection (hpi). Remdesivir (0.05 μmol/L) as a positive control. (B) Carrimycin did not inhibit the activities of viral replicases. SARS-CoV-2 $3CL^{pro}$ and RdRp activities were detected using sandwich-like FP and fluorometric assay, respectively. PF-07321332 or C646 as an individual positive control. Data are shown as mean ± SD (n = 3). (C) Proteomics sequencing. Huh7 cells were infected with hCoV-229E (MOI = 0.88) and treated with 5 μmol/L carrimycin. After 24 or 36 h, cell lysates were subjected to tandem mass tag (TMT) proteomic sequencing. The protein ratio of RdRp/$3CL^{pro}$ was calculated. (D) Ribosome profiling sequencing. Ribosome profiling sequencing (Ribo-seq) read counts within the genome of hCoV-229E gp1 (ORF1ab) in Huh7 cells infected with hCoV-229E (MOI = 0.88) and treated with carrimycin for 24 h. The relative translation ratios of ORF1b-to ORF1a-translated proteins and RdRp to $3CL^{pro}$ were calculated. P values were calculated using Student's t-test (mean ± SD, n = 3). *P < 0.05, **P < 0.01, and ns, P > 0.05 *vs*. control.

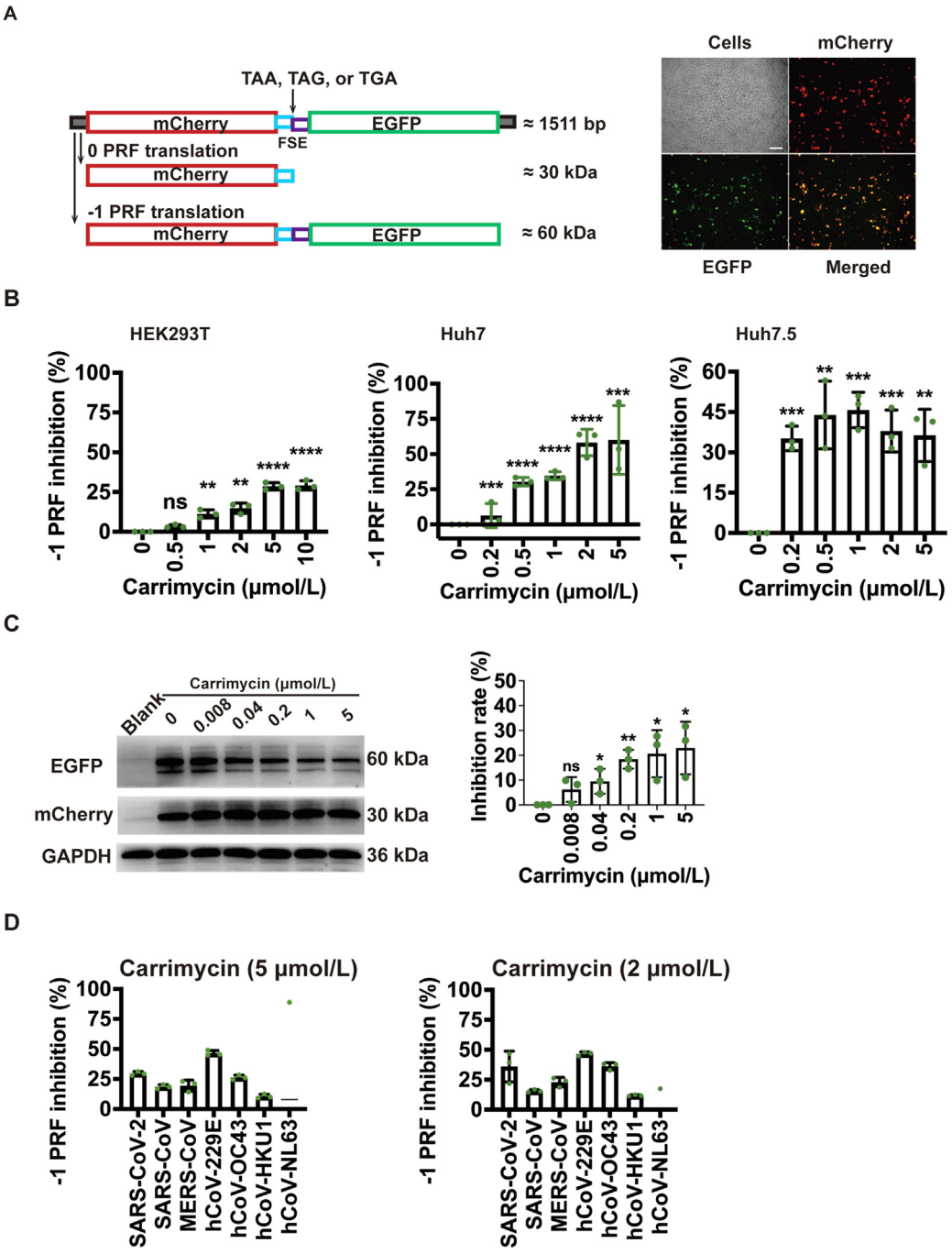

Figure 3 Carrimycin decreases the efficiency of −1 PRF of coronaviral RNAs. (A) The principle of the dual fluorescent reporter system showed the translational outcome, and the fluorescent density of mCherry and EGFP was visualized. Scale bar: 200 μm. (B) Carrimycin reduced the efficacy of −1 PRF of SARS-CoV-2 FSE detected by the fluorescent intensity at 24 h of drug treatment in HEK293T, Huh7, and Huh7.5 cells. The efficiency of −1 PRF was quantified by the ratio of EGFP to mCherry fluorescence intensity described in Method. (C) Inhibition on −1 PRF of SARS-CoV-2 by carrimycin in a rabbit reticulocyte lysate translation system. The efficiency of −1 PRF was quantified by the protein ratio of mCherry-EGFP to mCherry. (D) Carrimycin reduced the efficacy of −1 PRF of coronaviral FSEs in Huh7 cells. *P* values were calculated using Student's *t*-test (mean ± SD, $n = 3$). $^{*}P < 0.05$, $^{**}P < 0.01$, $^{***}P < 0.001$, and $^{****}P < 0.0001$ *vs*. control. −1 PRF, programmed −1 ribosomal frameshifting.

system, carrimycin also showed an inhibitory effect on the efficacy of −1 PRF (Fig. 3C), suggesting that carrimycin might directly inhibit the efficiency of −1 PRF of SARS-CoV-2.

Of the seven hCoVs known to infect humans[1], SARS-CoV, Middle East respiratory syndrome coronavirus (MERS-CoV), and SARS-CoV-2, the three newly-emerged viruses in the last two decades, have caused severe and fatal respiratory diseases accompanied by complications[1]. Therefore, we tested the inhibitory effect of carrimycin on the efficiency of −1 PRFs, which is controlled by the different coronaviral FSE RNAs (Supporting

Information Table S1). The results showed that carrimycin decreased the efficacy of the −1 PRFs controlled by the different FSEs of the three highly pathogenic coronaviruses and the common coronaviruses hCoV-229E, hCoV-OC43, or hCoV-HKU1 (Fig. 3D), demonstrating a broad-spectrum activity of carrimycin against coronaviruses in multiple cell lines[16].

3.4. *Carrimycin binds directly to viral FSE RNA pseudoknots*

To investigate the mode of action of carrimycin on the −1 PRF, we used surface plasmon resonance (SPR) spectroscopy to examine whether carrimycin interacts directly with coronaviral FSE RNA. SARS-CoV-2 FSE RNA was prepared from plasmids using the T7 promoter transcription system. RNA was biotinylated at 3′ poly(A) and captured with the streptavidin on a carboxymethylated dextran chip, and a carrimycin-bound FSE RNA signal was detected using Reichert 4-SPR system (Fig. 4A). Merafloxacin did not directly bind to SARS-CoV-2 FSE RNA (Fig. 4B), while carrimycin bound to the SARS-CoV-2 FSE RNA but not to non-FSE-related RNA (Fig. 4B). Similarly, carrimycin is also bound to the mCherry-SARS-CoV-2 FSE-EGFP chimeric RNA (Supporting Information Fig. S3A), suggesting that the specific viral FSE RNA sequence is the component responsible for the interaction between the virus and carrimycin. To validate the interaction between carrimycin and FSE RNA, we utilized isothermal titration calorimetry (ITC). The result showed that carrimycin interacted with FSE RNA (Fig. 4C, left), while remdesivir, an RdRp inhibitor, had no interaction (Fig. 4C, middle). Certainly, carrimycin did not interact with the non-related FES RNA (Fig. 4C, right), further suggesting the specific binding between carrimycin and SARS-CoV-2 FSE RNA. Carrimycin also bound directly to other coronaviral FSE RNAs with different binding affinity profiles, with the exception of hCoV-NL63 FSE RNA (Fig. S3B), further supporting the broad-spectrum antiviral activities of carrimycin. The results were further validated by the fact that hCoV-NL63 is resistant to carrimycin (Supporting Information Fig. S4). For further investigating the binding of carrimycin to viral FSE *in vivo*, a dimethyl sulfate mutational profiling with sequencing (DMS-MaPseq) was carried out in Huh7 cells infected with hCoV-229E. After treatment with carrimycin, DMS reactivities were decreased in the slippery sequence, stem-loop (SL) 1, SL2, and SL3 region (Fig. 4D), suggesting that carrimycin still binds strongly to the viral FSE *in vivo*.

To our knowledge, carrimycin might be the first antiviral agent that targets viral-specific RNA in laboratory tests. Therefore, the molecular detail of carrimycin has been further investigated. The unique α- and β-coronaviral FSE RNA signal shares a typical RNA pseudoknot structure consisting of a heptameric slippery sequence (UUUAAAC), a short spacer, and a 3-stem-loop architecture (Fig. 4E)[26], although the FSE RNA sequences in coronaviruses are not the same (Supporting Information Table S1 and Fig. S5A). Next, we investigated the potential binding model between carrimycin and FSE RNA. Based on the elements of RNA pseudoknot, the truncated mutants of the RNA sequences were prepared (Fig. 4E, Table S2), and the binding affinities with carrimycin were analyzed. Interestingly, the binding affinity with carrimycin vanished after deletion of the slippery sequence or any of the RNA stems (Fig. 4F), suggesting that the binding of carrimycin with the specific RNA seems to be associated with the RNA pseudoknot stereostructure but not the RNA linear structure, which agrees with the DMS-MaPseq results (Fig. 4D).

To further validate whether the binding of FSE RNA is the antiviral mechanism of carrimycin, we carried out a rescue experiment. Huh7 cells were transfected with SARS-CoV-2 FSE RNA, then infected with hCoV-229E and treated with carrimycin. siRNA targeting the FSE RNA of hCoV-229E inhibited the replication of hCoV-229E (Supporting Information Fig. S6), further demonstrating that targeting FSE RNA is a new strategy for interrupting the replication of hCoVs. The inhibitory activity of carrimycin against hCoV-229E was reduced by the addition of exogenous SARS-CoV-2 FSE RNA, while not by the exogenous negative control hCoV-NL63 FSE RNA (Fig. 4G), suggesting that the active amount of carrimycin to bind the FSE RNA of hCoV-229E is reduced by the binding of carrimycin to the exogenous SARS-CoV-2 FSE RNA. These results hint that carrimycin restrains viral replication through direct binding to viral FSE RNA.

3.5. *Carrimycin synergistically enhances the antiviral activities of viral replicase inhibitors*

Considering the unique antiviral mechanism of carrimycin, we speculated that carrimycin is a potential antiviral agent in combination with the known viral replicase inhibitors. Indeed, in the Huh7 cells, carrimycin combined with remdesivir (Fig. 5A), molnupiravir (Fig. 5B), or nirmatrelvir (Fig. 5C) synergistically inhibited hCoV-229E replication. Similarly, in the H460 cells, carrimycin plus molnupiravir (Fig. 5D) or plus azvudine (Fig. 5E), an RdRp inhibitor approved for the treatment of SARS-CoV-2 in China[4], also showed a synergistic inhibitory effect against hCoV-OC43. These results suggest that targeting viral FSE RNA might be a new strategy for developing new and rationally designed combination therapies for various coronaviruses.

4. Discussion

In summary, we demonstrate that carrimycin decreases the efficiency of −1 PRF by binding directly to the conserved viral FSE RNA pseudoknot, resulting in the arrest of the viral protein translation switch from ORF1a to ORF1b, which reduces the amount of core components of viral replication and transcription complexes, causing an interruption of viral replication. Because the antiviral mechanism is new and unique, carrimycin showed synergistic antiviral effects in combination with viral replicase inhibitors (Fig. 6).

In several RNA viruses, including members of the *Coronaviridae*, *Retroviridae*, *Totiviridae*, and *Luteoviridae* families, −1 PRF signal highly regulates the relative expression level of different proteins encoded in the same viral RNA genome in time to maintain optimal stoichiometry for productive infection[30]. In the *Coronaviridae* family, the translation of ORF1a and ORF1b is accurately controlled by −1 PRF signal[31]. Maintaining the precise level of coronavirus frameshifting efficiency is crucial for viral replication, and changes in efficiency are detrimental to viral viability and infectivity[28]. In SARS-CoV, a ∼3.5-fold reduction of −1 PRF efficiency was shown to cause an over 1000-fold attenuation of the viral replication[32], which may be why an approximately 31% decrease in ribosome profiling appears to have a good antiviral effect of carrimycin. However, the inhibition activities of carrimycin on the frameshifting efficiency measured

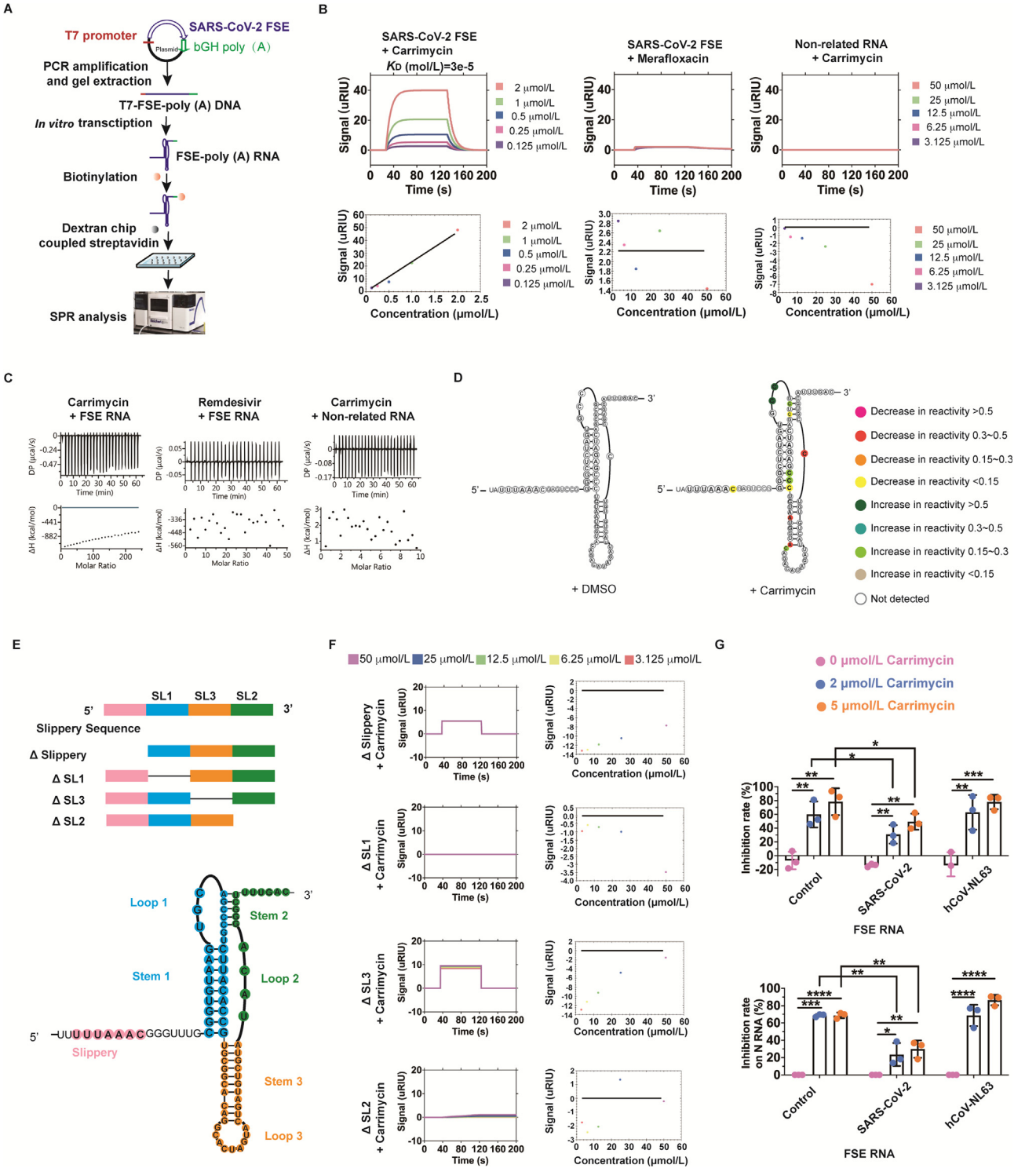

Figure 4 Carrimycin binds directly to viral FSE RNA pseudoknots. (A) Methodology for detecting affinity between the compound and FSE RNA. (B) Affinity between the compound and SARS-CoV-2 FSE RNA. (C) Interaction between carrimycin and FSE RNA detected by ITC. Up panel: power required to maintain the temperature of the RNA solution (baseline-corrected). Down panel: integrated heats of interaction plotted against the molar ratio of ligand over RNA and fitted to a single binding site model (MicroCal PEAQ-ITC Analysis Software 1.1.0). (D) DMS-Map upon carrimycin binding in Huh7 cells infected with hCoV-229E. FSE RNA pseudoknot structure (left) and average changes ($n = 2$) in DMS reactivity upon carrimycin binding (right). Colored nucleotides represent a decrease or increase in reactivity. (E) The typical structure of SARS-CoV-2 FSE RNA pseudoknot and truncated mutations of FSE RNAs. (F) The affinity between carrimycin and FSE RNA with truncated mutations. (G) Exogenous SARS-CoV-2 FSE RNA reduced the antiviral activity of carrimycin against hCoV-229E in Huh7 cells detected with CCK-8 staining assay (up) and qRT-PCR (down) methods ($n = 3$). P values were calculated using Student's t-test (mean ± SD). $^*P < 0.05$, $^{**}P < 0.01$, $^{***}P < 0.001$, $^{****}P < 0.0001$ and ns, $P > 0.05$ *vs*. control.

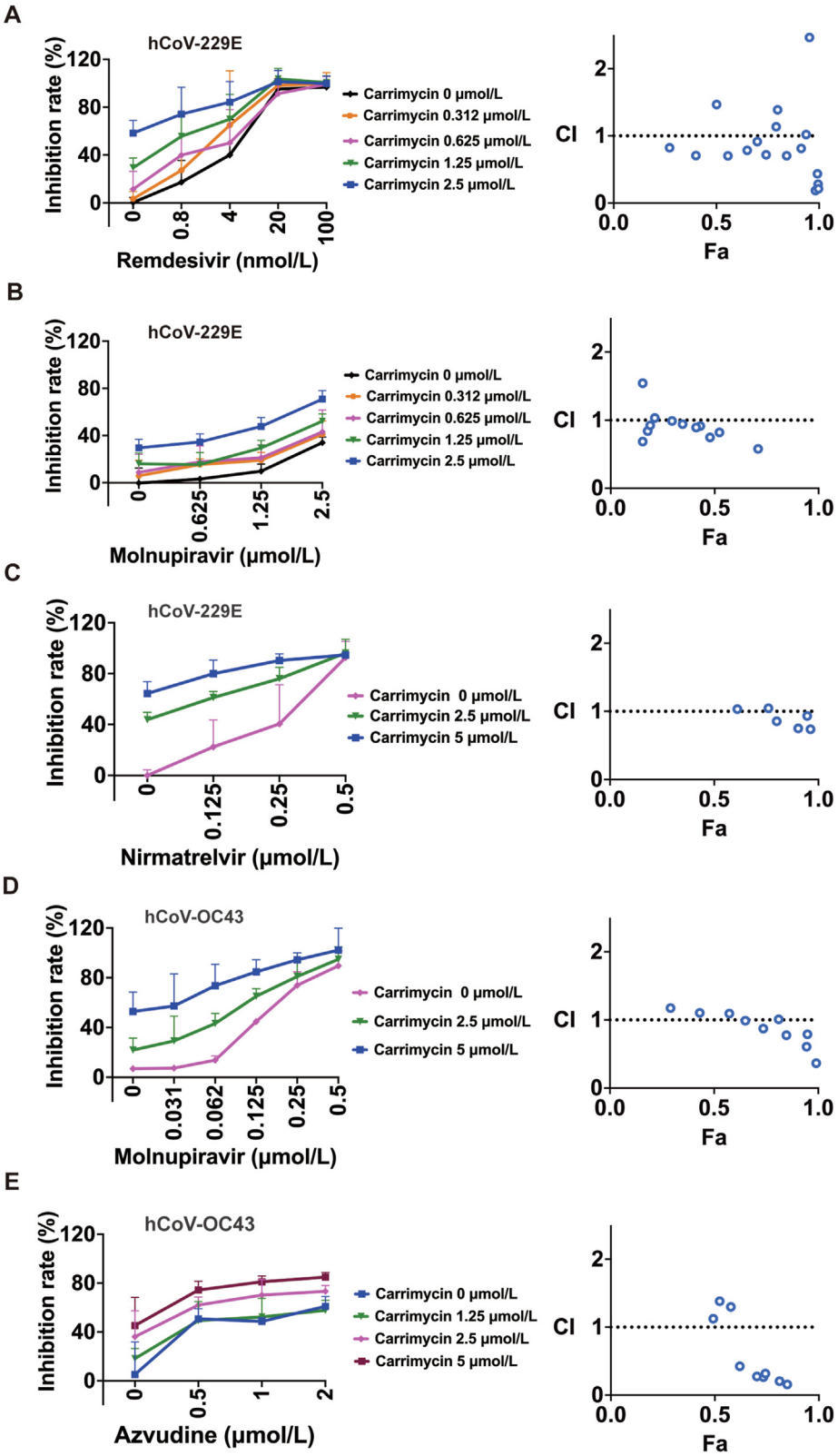

Figure 5 Carrimycin synergistically enhances the antiviral activities of viral replicase inhibitors. (A–C) Carrimycin in combination with remdesivir (A), molnupiravir (B), or nirmatrelvir (C) synergistically inhibited hCoV-229E (MOI = 0.05) replication in Huh7 cells. (D) Carrimycin in combination with molnupiravir synergistically inhibited hCoV-OC43 (MOI = 1) replication. Cells were infected with the virus and treated simultaneously with compounds. At 72 h, the cell viability was detected by CCK-8 assay, and antiviral activities were calculated. Data are shown as mean ± SD (n = 3). (E) Carrimycin plus azvudine synergistically inhibited hCoV-OC43 using qRT-PCR (RdRp RNA). The combination index (CI) was calculated by the Chou-Talalay method using CompuSyn version 1.0, where CI > 1 indicates antagonism, CI = 1 indicates addition, and CI < 1 suggests synergy between the two drugs. Fa, inhibition of test compounds combination.

by the dual fluorescent reporter, proteomic sequencing, and ribosome profiling were somewhat different, which might be caused by the different sensitivity of the different methods. In addition, other elements of coronavirus and hosts might also influence the FSE efficiency[26], which needs further investigation. All those clues suggested that the −1 PRF machinery is essential for all coronaviruses and is a rate-limiting step in SARS-CoV-2 replication. Furthermore, the −1 PRF signal is evolutionarily highly conserved in the SARS-CoV family, especially with the typical three stem-loops hairpin-type pseudoknot[33], which is not the case for host cellular mRNAs[33]. Also, up to date, the FSE sequences are highly conserved with no nucleotide mutants in the variants of concern of SARS-CoV-2 (Fig. S5B). In addition, the region of the frameshifting element had a generally low ribosome density compared to the surrounding sequences throughout the infection[34], suggesting that a compound will be relatively easy to access the RNA binding site once it enters into cells. Thus, the −1 PRF machinery in coronaviruses may be a good target for developing broad-spectrum antivirals.

Combined antiviral therapy with multi-targets contributes to addressing antiviral drug resistance. Currently, several candidates, which mainly target viral protease and RdRp, have been in phase III clinic trials for the treatment of the SARS-CoV-2 infection[35], and several RdRp inhibitors and 3CL^{pro} inhibitors are available for clinical use[2–7,11,36]. Due to the characteristics of viral replication, the emergence of drug-resistant mutations is inevitable[37], showing that the viral load rebounded in some patients after Paxlovid treatment[38]. Because the mechanism of action of carrimycin against coronavirus is different from that of RdRp and protease inhibitors, their combined use may produce a synergistic antiviral activity by down-regulating the amount or activity of the viral replication and transcription complexes at different stages (Fig. 6). Our results demonstrated that carrimycin exhibited a synergistic effect when combined with remdesivir, molnupiravir, nirmatrelvir, or azvudine, suggesting that the combined strategy is practicable. Because carrimycin is also a clinically used drug, its combined use with replicase inhibitors is worth expecting to defend the variants of concern of SARS-CoV-2. Indeed, carrimycin showed inhibitory activity against the SARS-CoV-2 Omicron strain in Vero-E6 cells at different multiplicities of infection (Fig. 1D) and SARS-CoV-2 wild-type strain[16].

Up to date, antiviral drugs have mainly targeted proteins, including enzymes, kinases, and receptors[39]. Due to many disease-related proteins being termed undruggable[40], if small-molecule therapeutics could be extended to target RNA, the landscape of targetable macromolecules would be expanded extremely[29]. Our results demonstrated that carrimycin binds directly to viral FSE RNA and thus decreases the efficacy of −1 PRF. Unlike standard antisense oligonucleotides, the binding model between carrimycin and FSE RNA might not be linear but based on the conserved viral

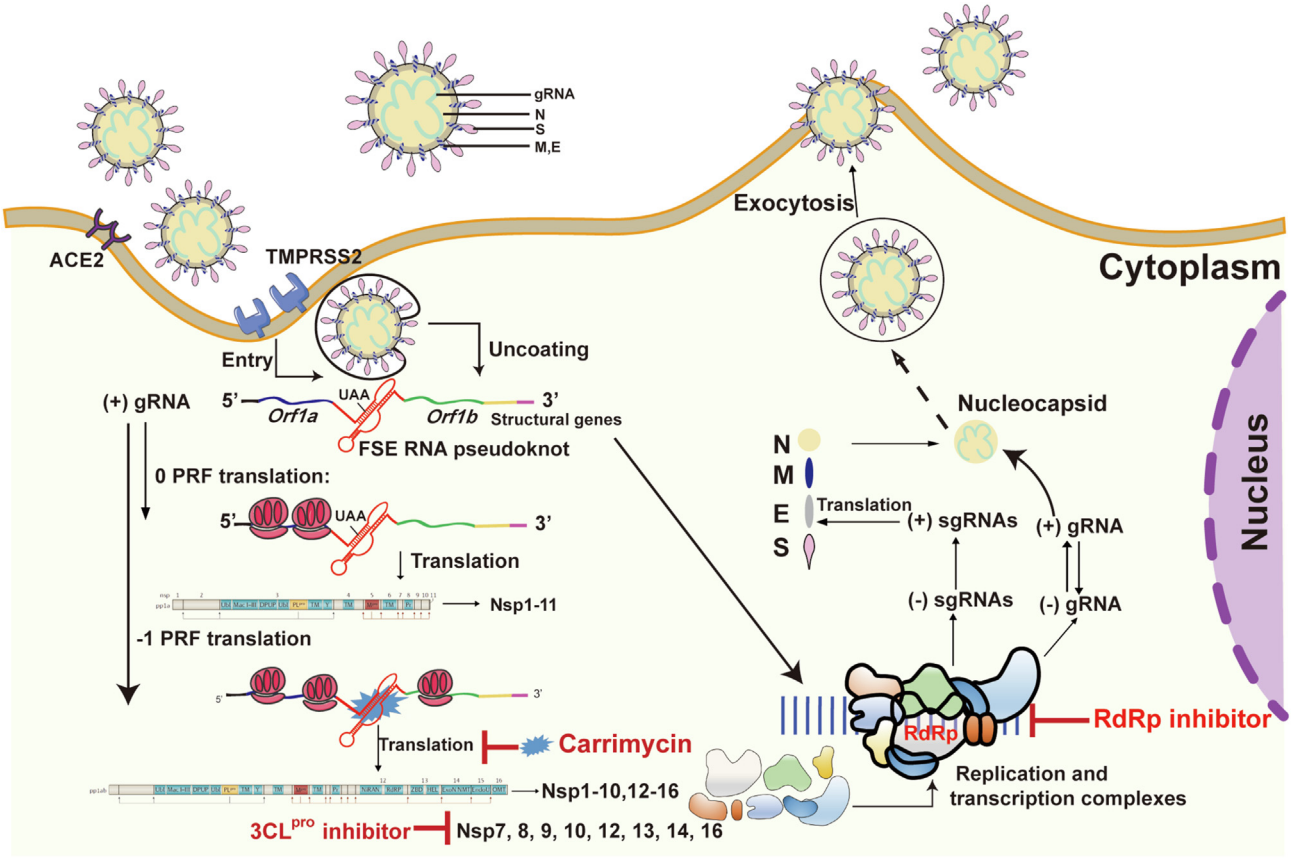

Figure 6 Overview of the mechanism of action and role of carrimycin against hCoV. Coronaviruses apply the −1 PRF mechanism to switch complete protein translation from ORF1a to ORF1b, while carrimycin binds directly to the coronaviral FSE RNA pseudoknot to stop the switch procedure and thus reduces the amount of viral encoded polyprotein, which is hydrolyzed by 3CL^{pro} into core components of viral replication and transcription complexes. Since carrimycin, 3CL^{pro} inhibitor, and RdRp inhibitor interrupt viral replication at different stages of the viral life cycle, the combination of carrimycin and them produces a synergistic inhibitory effect on coronaviruses.

RNA pseudoknot stereostructure (Fig. S5), which may guide us to perform structure−activity relationship analysis to find innovative drug candidates with better activity and broader antiviral-spectrum, especially in combination with the potential Cryo-EM structure of viral FSE RNA and carrimycin. Therefore, the action mode of carrimycin has also opened up a new model for the discovery of RNA drugs, which is of great significance for the development of innovative antiviral drugs in the future.

5. Conclusions

In conclusion, this study on the mechanism of action of carrimycin identifies the pseudoknot stereostructure of coronavirus FSE RNA as a novel antiviral target. It is very different from the known antivirals that mainly target viral proteins. If the coronaviral FSE RNA sequence could be further verified as an antiviral target, we might enter a new frontier in discovering innovative antivirals.

Acknowledgments

We thank Dr. Lin-lin Bao and Prof. Chuan Qin for the test and analysis of the antiviral activity of carrimycin against the SARS-CoV-2 Omicron strain. We also thank Cloudseq Biotech Inc. (Shanghai, China) and Oebiotech Co., Ltd. (Shanghai, China) for the high throughput sequencing service and bioinformatic support. This work was supported by grants from the National Natural Science Foundation, China (82151525), the National key research and development program, China (2022YFC0869000), and the CAMS Innovation Fund for Medical Sciences (2022-I2M-JB-013, 2021-I2M-1-028 and 2022-I2M-2-002, China).

Author contributions

Hongying Li, Jianrui Li, Zonggen Peng, Yongsheng Che, and Jian-Dong Jiang conceived the project; Hongying Li, Jianrui Li, Bin Hong, Shuyi Si, Zonggen Peng, and Jian-Dong Jiang designed the experiments; Hongying Li, Jianrui Li, Hu Li, Jiayu Li, Jing Jiang, Lei Lei, Han Sun, Mei Tang, and Biao Dong carried out the experiments; Hongying Li, Jianrui Li, Xuekai Wang, Bin Hong, Shuyi Si, Jian-Dong Jiang, and Zonggen Peng analyzed the data and provided advice on the interpretation of data; Weiqing He, Yinghong Li, and Danqing Song provided essential reagents; Hu Li, Zonggen Peng, Yongsheng Che, and Jian-Dong Jiang acquired funding; Hongying Li, Jianrui Li, Bin Hong, Shuyi Si, Zonggen Peng, and Jian-Dong Jiang wrote the original draft; Zonggen Peng and Jian-Dong Jiang wrote the final draft; all authors approved the final manuscript.

Conflicts of interest

The authors declare no conflicts of interest.

Appendix A. Supporting information

Supporting data to this article can be found online at https://doi.org/10.1016/j.apsb.2024.02.023.

References

1. Kung YA, Lee KM, Chiang HJ, Huang SY, Wu CJ, Shih SR. Molecular virology of SARS-CoV-2 and related coronaviruses. *Microbiol Mol Biol Rev* 2022;**86**:e0002621.
2. Food and Drug Administration. Coronavirus (COVID-19)|Drugs. 2023. Available from: https://www.fda.gov/drugs/emergency-preparedness-drugs/coronavirus-covid-19-drugs.
3. Syed YY. Molnupiravir: first approval. *Drugs* 2022;**82**:455−60.
4. Zhang JL, Li YH, Wang LL, Liu HQ, Lu SY, Liu Y, et al. Azvudine is a thymus-homing anti-SARS-CoV-2 drug effective in treating COVID-19 patients. *Signal Transduct Targeted Ther* 2021;**6**:414.
5. Cao ZJ, Gao WY, Bao H, Fenng HY, Mei SY, Chen PZ, et al. VV116 *versus* nirmatrelvir−ritonavir for oral treatment of Covid-19. *N Engl J Med* 2023;**388**:406−17.
6. Lamb YN. Nirmatrelvir plus ritonavir: first approval. *Drugs* 2022;**82**:585−91.
7. Mukae H, Yotsuyanagi H, Ohmagari N, Doi Y, Sakaguchi H, Sonoyama T, et al. Efficacy and safety of ensitrelvir in patients with mild-to-moderate coronavirus disease 2019: the phase 2b part of a randomized, placebo-controlled, phase 2/3 study. *Clin Infect Dis* 2023;**76**:1403−11.
8. Ji X, Meng X, Zhu X, He Q, Cui Y. Research and development of Chinese anti-COVID-19 drugs. *Acta Pharm Sin B* 2022;**12**:4271−86.
9. Lyu M, Fan G, Xiao G, Wang T, Xu D, Gao J, et al. Traditional Chinese medicine in COVID-19. *Acta Pharm Sin B* 2021;**11**:3337−63.
10. Mittal A, Khattri A, Verma V. Structural and antigenic variations in the spike protein of emerging SARS-CoV-2 variants. *PLoS Pathog* 2022;**18**:e1010260.
11. Wang YM, Zhang DY, Du GH, Du RH, Zhao JP, Jin Y, et al. Remdesivir in adults with severe COVID-19: a randomised, double-blind, placebo-controlled, multicentre trial. *Lancet* 2020;**395**:1569−78.
12. Kiso M, Yamayoshi S, Iida S, Furusawa Y, Hirata Y, Uraki R, et al. *In vitro* and *in vivo* characterization of SARS-CoV-2 resistance to ensitrelvir. *Nat Commun* 2023;**14**:4231.
13. Brown A, Lang Y, Zhou J, Franco EJ, Hanrahan KC, Bulitta J, et al. Why molnupiravir fails in hospitalized patients. *mBio* 2022;**13**:e0291622.
14. Carlin AF, Clark AE, Chaillon A, Garretson AF, Bray W, Porrachia M, et al. Virologic and immunologic characterization of coronavirus disease 2019 recrudescence after nirmatrelvir/ritonavir treatment. *Clin Infect Dis* 2023;**76**:e530−2.
15. Kesheh MM, Hosseini P, Soltani S, Zandi M. An overview on the seven pathogenic human coronaviruses. *Rev Med Virol* 2022;**32**:e2282.
16. Yan H, Sun J, Wang K, Wang H, Wu S, Bao L, et al. Repurposing carrimycin as an antiviral agent against human coronaviruses, including the currently pandemic SARS-CoV-2. *Acta Pharm Sin B* 2021;**11**:2850−8.
17. Jin Y, Zuo HX, Li MY, Zhang ZH, Xing Y, Wang JY, et al. Anti-tumor effects of carrimycin and monomeric isovalerylspiramycin I on hepatocellular carcinoma *in vitro* and *in vivo*. *Front Pharmacol* 2021;**12**:774231.
18. ClinicalTrials.gov. Study to evaluate safety and efficacy of carrimycin for treatment of severe coronavirus disease 2019 (COVID-19) in hospitalized patients. 2020. Available from: https://clinicaltrials.gov/study/NCT04672564.
19. Yu KJ. A multicenter, randomized, open, controlled trial for the efficacy and safety of oral kolimycin in the treatment of patients with new coronavirus pneumonia (COVID-19). 2020. Available from: https://www.chictr.org.cn/showproj.html?proj=52824.
20. Irigoyen N, Firth AE, Jones JD, Chung BY, Siddell SG, Brierley I. High-resolution analysis of coronavirus gene expression by RNA sequencing and ribosome profiling. *PLoS Pathog* 2016;**12**:e1005473.
21. Bai X, Sun H, Wu S, Li Y, Wang L, Hong B. Identifying small-molecule inhibitors of SARS-CoV-2 RNA-dependent RNA

polymerase by establishing a fluorometric assay. *Front Immunol* 2022;**13**:844749.
22. Yan G, Li D, Lin Y, Fu Z, Qi H, Liu X, et al. Development of a simple and miniaturized sandwich-like fluorescence polarization assay for rapid screening of SARS-CoV-2 main protease inhibitors. *Cell Biosci* 2021;**11**:199.
23. Groher F, Bofill-Bosch C, Schneider C, Braun J, Jager S, Geißler K, et al. Riboswitching with ciprofloxacin-development and characterization of a novel RNA regulator. *Nucleic Acids Res* 2018;**46**:2121−32.
24. K A, Sharma A, Kumar D, Singh SK, Gupta G, Chellappan DK, et al. Molecular aspects of Omicron, vaccine development, and recombinant strain XE: a review. *J Med Virol* 2022;**94**:4628−43.
25. Vázquez-Laslop N, Mankin AS. How macrolide antibiotics work. *Trends Biochem Sci* 2018;**43**:668−84.
26. Zimmer MM, Kibe A, Rand U, Pekarek L, Ye L, Buck S, et al. The short isoform of the host antiviral protein ZAP acts as an inhibitor of SARS-CoV-2 programmed ribosomal frameshifting. *Nat Commun* 2021;**12**:7193.
27. Sun Y, Abriola L, Niederer RO, Pedersen SF, Alfajaro MM, Silva Monteiro V, et al. Restriction of SARS-CoV-2 replication by targeting programmed −1 ribosomal frameshifting. *Proc Natl Acad Sci U S A* 2021;**118**:e2023051118.
28. Bhatt PR, Scaiola A, Loughran G, Leibundgut M, Kratzel A, Meurs R, et al. Structural basis of ribosomal frameshifting during translation of the SARS-CoV-2 RNA genome. *Science* 2021;**372**:1306−13.
29. Warner KD, Hajdin CE, Weeks KM. Principles for targeting RNA with drug-like small molecules. *Nat Rev Drug Discov* 2018;**17**:547−58.
30. Huang X, Cheng Q, Du Z. A genome-wide analysis of RNA pseudoknots that stimulate efficient −1 ribosomal frameshifting or readthrough in animal viruses. *BioMed Res Int* 2013;**2013**:984028.
31. Kadam SB, Sukhramani GS, Bishnoi P, Pable AA, Barvkar VT. SARS-CoV-2, the pandemic coronavirus: molecular and structural insights. *J Basic Microbiol* 2021;**61**:180−202.
32. Plant EP, Rakauskaite R, Taylor DR, Dinman JD. Achieving a golden mean: mechanisms by which coronaviruses ensure synthesis of the correct stoichiometric ratios of viral proteins. *J Virol* 2010;**84**:4330−40.
33. Kelly JA, Woodside MT, Dinman JD. Programmed −1 ribosomal frameshifting in coronaviruses: a therapeutic target. *Virology* 2021;**554**:75−82.
34. Puray-Chavez M, Lee N, Tenneti K, Wang Y, Vuong HR, Liu Y, et al. The translational landscape of SARS-CoV-2-infected cells reveals suppression of innate immune genes. *mBio* 2022;**13**:e0081522.
35. Rahmah L, Abarikwu SO, Arero AG, Essouma M, Jibril AT, Fal A, et al. Oral antiviral treatments for COVID-19: opportunities and challenges. *Pharmacol Rep* 2022;**74**:1255−78.
36. Bernal AJ, Gomes da Silva MM, Musungaie DB, Kovalchuk E, Gonzalez A, Reyes VD, et al. Molnupiravir for oral treatment of Covid-19 in nonhospitalized patients. *N Engl J Med* 2022;**386**:509−20.
37. Heyer A, Günther T, Robitaille A, Lütgehetmann M, Addo MM, Jarczak D, et al. Remdesivir-induced emergence of SARS-CoV2 variants in patients with prolonged infection. *Cell Rep Med* 2022;**3**:100735.
38. Wang Y, Chen X, Xiao W, Zhao D, Feng L. Rapid COVID-19 rebound in a severe COVID-19 patient during 20-day course of Paxlovid. *J Infect* 2022;**85**:e134−6.
39. Sadremomtaz A, Al-Dahmani ZM, Ruiz-Moreno AJ, Monti A, Wang C, Azad T, et al. Synthetic peptides that antagonize the angiotensin-converting enzyme-2 (ACE-2) interaction with SARS-CoV-2 receptor binding spike protein. *J Med Chem* 2022;**65**:2836−47.
40. Tanaka T, Williams RL, Rabbitts TH. Tumour prevention by a single antibody domain targeting the interaction of signal transduction proteins with RAS. *EMBO J* 2007;**26**:3250−9.